ELSEVIER

Chemical Engineering Journal 118 (2006) 153–159

Chemical Engineering Journal

www.elsevier.com/locate/cej

Fluidized bed photoreactors using composites of titania CVD-coated onto quartz sand as photocatalyst: Assessment of photochemical efficiency

Roberto L. Pozzo, Rodolfo J. Brandi, José L. Giombi, Alberto E. Cassano, Miguel A. Baltanás *

INTEC, Instituto de Desarrollo Tecnológico para la Industria Química, Universidad Nacional del Litoral and CONICET, Güemes 3450, S3000GLN Santa Fe, Argentina

Received 10 August 2005; received in revised form 20 December 2005; accepted 26 January 2006

Abstract

The photochemical efficiency of a fluidized bed (FB) of quartz sand coated with TiO_2 by plasma-CVD, was investigated using a fully illuminated, parallel planar photoreactor. The local volumetric rate of photon absorption (LVRPA) of the device was obtained by the combined use of experimental measurements and computer modeling of the radiation field. Because of the anisotropy of the FB in the vertical direction, due to particle segregation, and the strong absorption of radiation of the photocatalyst particles across the photoreactor, a two-dimensional modeling (2D) was developed. To accomplish these goals, the relevant *specific* volumetric optical parameters (namely, the spectral absorption and scattering coefficient) of FBs of the TiO_2-coated quartz catalytic composite were used. To take into account said vertical anisotropy of the fluidized bed, a functional dependency between the spectral optical coefficients and bed height was derived in the present work, by assuming a completely segregated FB, and experimentally validated through transmittance measurements. Finally, the evaluation of the photochemical efficiency of the FB in the decomposition of oxalic acid, a well-known model reactant, revealed that this type of devices might outperform the conventional slurry systems, as well as dispense of downstream separation steps.

Keywords: Fluidized bed; Supported photocatalysts and radiation field modeling

1. Introduction

Fluidization of photocatalytically active materials to eliminate water pollutants with UV irradiation arises as an interesting, convenient alternative versus the slurried systems of finely powdered photocatalyst that, in most cases, require the additional cost of downstream separation steps.

In both cases, the description and evaluation of the radiation field inside the reaction volume is a prerequisite for achieving a significant kinetic modeling of the photocatalytic process and/or for reactor design purposes. This implies that the local values of the radiation intensity at each point of the reaction volume must be obtained, by solving the radiation transfer equation (RTE). Since the analytical solution of the RTE is not usually workable, numerical integration is an alternative but, in either case, the knowing of the spectral volumetric scattering and absorption coefficients (k_λ and σ_λ) of the absorbing media is unavoidable.

These optical properties can be considered as spatially uniform in a slurry. However, that is not usually the case for a realistic fluidized bed (FB), which usually have particles of different sizes. Therewith, in order to model the radiation field in this kind of systems, a relationship among optical properties and particle(s) location inside the FB must be found.

It is well-known that sedimentation of particles with different sizes or densities produce vertical anisotropy in FBs, which implies different optical properties, and may significantly affect the radiation field, in the vertical direction.

Yue and coworkers studied and modeled this type of field anisotropy in a flat photoreactor, for a gas–solid fluidized bed [1–3]. However, gas bubbles – that seem to play an important role in the particles mixing – are absent in liquid–solid FBs. Bhargava et al. [4] analyzed the performance of a photocatalytic, annular FB reactor for the treatment of wastewater. By utilizing radioactive particles and two perpendicularly arranged γ-ray cameras

* Corresponding author. Tel.: +54 342 455 9175; fax: +54 342 455 0944.
E-mail address: tderliq@ceride.gov.ar (M.A. Baltanás).

1385-8947/$ – see front matter © 2006 Elsevier B.V. All rights reserved.
doi:10.1016/j.cej.2006.01.014

Nomenclature

A	empty bed cross-sectional area (m^2)
$C_{Ox}(t)$, C_{Ox}^{O}	oxalic acid concentration as a function of time, initial oxalic acid concentration ($mol\,m^{-3}$)
D_p	nominal particle diameter (m)
$e^{a}_{(x,y)}$	local volumetric rate of radiation photon absorption (Einstein $m^{-3}\,s^{-1}$)
E	global bed expansion (expanded bed volume/unexpanded bed volume)
E_h	local bed expansion at bed height h
$G_{x,y}$	total local incident radiation (Einstein $m^{-2}\,s^{-1}$)
H_R	fluidized bed height (m)
I_λ	monochromatic specific radiation intensity (Einstein $m^{-2}\,s^{-1}\,sr^{-1}$)
$I^{o}_{\lambda,\underline{\Omega}}$	monochromatic specific radiation intensity, on the reactor window, at $\underline{\Omega}$ direction ($m^{-2}\,s^{-1}\,sr^{-1}$)
k_λ, k^*_λ	spectral absorption coefficient, specific spectral absorption coefficient (m^{-1})
$m(D_p)$	differential (diameter averaged) mass distribution function of the particulate material
Re_t	particle Reynolds number ($U_t D_p \rho_f/\mu$)
$\langle R^{O}_{Ox}(x,y)\rangle$	volume-averaged initial reaction rate ($mol\,m^{-3}\,s^{-1}$)
U_o	superficial velocity ($m\,s^{-1}$)
U_t	particle terminal velocity ($m\,s^{-1}$)
V_R	fluidized bed reaction volume (m^3)
V_T	volume of reservoirs tanks in the recirculating system, outside the V_R (m^3)

Greek letters

ε, ε_o	overall voidage, unexpanded bed overall voidage
ε_h	voidage at bed height h
μ	fluid viscosity, Pa s ($kg\,m^{-1}\,s^{-1}$)
ρ_f	fluid density ($kg\,m^{-3}$)
ρ_s	solid density ($kg\,m^{-3}$)
σ_λ, σ^*_λ	spectral scattering coefficient, specific spectral scattering coefficient (m^{-1})
$\underline{\Omega}'$	unit vector in the direction of propagation

these authors were able to map and correlate the solid voidage and fluidodynamics of the FB with both, the probability of a particle being in an irradiated zone, and the reaction kinetics. They did not attempt to measure the optical properties of the fluidized bed, though.

As regards the dynamics of the solid–liquid media in the FB, using beads with just two different sizes Kennedy and Bretton [5] proposed that two opposing mechanisms are simultaneously interacting in the system: a 'diffusion mechanism' which promotes random mixing versus a 'classification mechanism', as a result of dissimilar sedimentation velocities. Along these lines Van der Meer et al. [6] worked on liquid FB using particles of different densities, but quite similar sizing, while Dutta et al. [7] and Di Felice et al. [8] investigated on liquid FB constituted by binary systems of particles with different size and/or density. Likewise, Al-Dibouni and Garside [9] worked on solid–liquid fluidized beds with a wide range of mixed particle sizes. By using the ratio of the largest to the smallest particle size (d_R), as an assessment criterion, they found that the mixing model is successful for any fluidized bed where $d_R < 2.2$, particularly if the FB voidage is close to 0.7. However, given the uncertainty involved in the calculation of the eddy diffusion coefficients, they arrived to the conclusion that in most practical situations, a more simple classification model allows to account for the particle size distribution along the FB satisfactorily.

This last criterion was adopted in the present work to establish the relationships among particle size, and local voidage versus FB height by assuming a completely segregated, size-classified fluidized bed (viz.: only one particle size can exist at each FB level). The local, spectral volumetric optical coefficients (k_λ and σ_λ) of a fluidized bed, constituted by a TiO_2-coated quartz sand photocatalytic composite, were then evaluated as a function of FB height. As pivot values, the corresponding *specific* optical coefficients determined at the central region of the bed using different FB expansions [10], were used.

Furthermore, the local volumetric rate of photon absorption (LVRPA) and its averaged value in the reaction volume (VRPA) were calculated by a proper solution of the radiation transfer equation (RTE) with the previously determined optical coefficients and by using a two-dimensional (2D) modeling for the radiation field. Furthest, the photochemical efficiency of the device on the decomposition of oxalic acid, a well-known model reactant, at a concentration level where zero order reaction can be assumed, was also evaluated.

2. Experimental

All the experiments were carried out using a planar reactor/cell constituted by a pair of optically clear 3.0 mm thick Tempax® borosilicate glass walls, each one respectively attached to both sides of a hollow frame of aluminum, allowing a 7.0 mm optical gap between the transparent windows. A grid of Teflon® divided the cell into two compartments: the upper one (21 cm high), where the fluidized beds of the TiO_2 quartz sand catalyst composite was allowed to develop, and the lower one filled with glass spheres, for lessening jet formation in the bed zone immediately above the grid. In all the experiments the expansion of the fluidized beds was seven times the unexpanded bed volume, using 20 g of the catalytic composite. The stabilization of the fluidized bed under the high liquid flow rate was achieved by means of a constant hydrostatic pressure generation device consisting of two 'open-atmosphere' recirculating loops which included two reservoir tanks, labeled as tank 2 (80 cm^3) and tank 3 (200 cm^3) in Fig. 1. Air bubbling throughout the photochemical experiments maintained a constant concentration of dissolved O_2 and mechanical agitation in the biggest reservoir tank assured a uniform concentration of the model reactant (oxalic acid) in the recirculating system, outside the reactor cell. Additional information about the FB recirculating system is given in a previous work [10].

The UV irradiation system consisted of a pair of tubular black light lamps (Philips TLD 18W/08; nominal output power: 18 W;

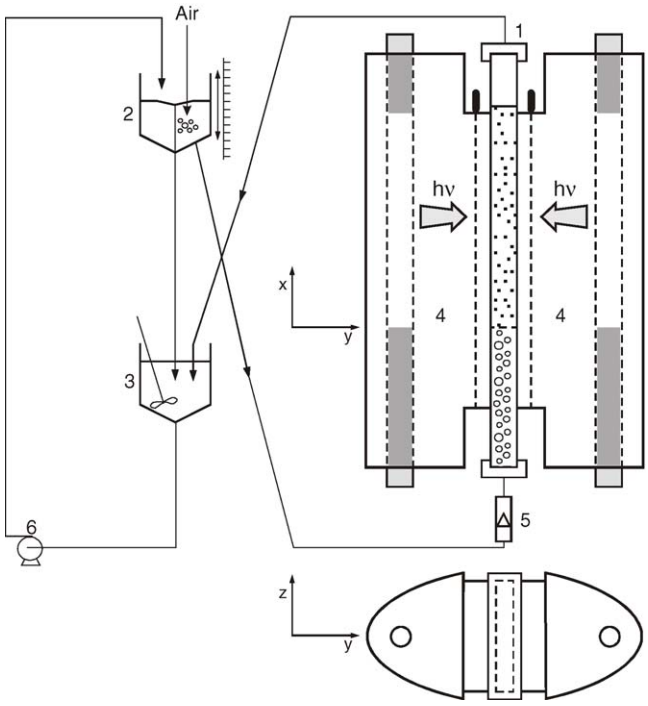

Fig. 1. Experimental set-up: (1) plane photoreactor/optical cell, (2) reservoir tank, (3) reservoir tank, (4) lamp-reflector illumination device, (5) flow meter, and (6) peristaltic pump.

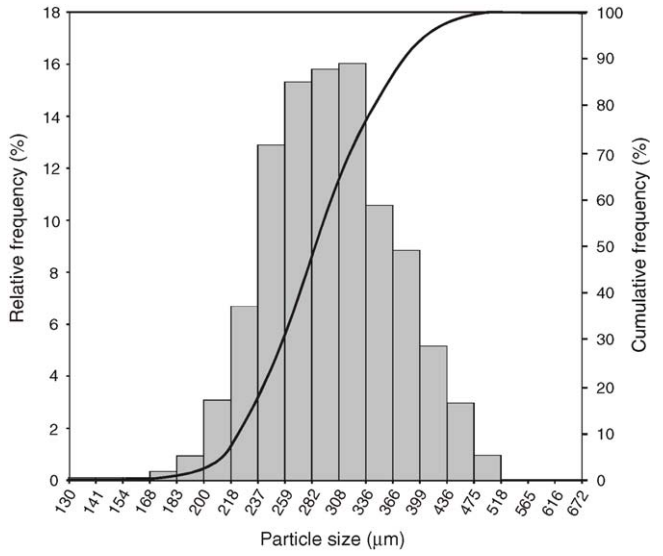

Fig. 2. Particle size distribution of the quartz sand, presented as a histogram of the per cent relative frequency as a function of the particle size and as the cumulative frequency of said particle sizes. The plotted particle size intervals were computer-generated from the micrography data.

superficial emission from 340 to 400 nm, with a peak at 365 nm). Within the lamp radiation spectral span, the calculated scattering and absorption coefficients were practically constant; i.e.: the FB behaves practically as a gray body with respect to both parameters. The lamps were situated lengthwise, one at each side of the cell, concurrent with the focal axis of two parabolic reflectors made of an aluminum sheet (Alzac treated) to collimate the rays (Fig. 1). In this way, both reactor windows were "quasi uniformly" irradiated. The incident radiation power from each lamp to the reactor windows was determined via actinometry by recirculating a 6×10^{-6} mol/cm^3 solution of potassium ferrioxalate through the reaction space. More details on these actinometric determination procedures can be found in a previous report [11].

The catalyst composite was prepared by low-temperature CVD-plasma coating of Aldrich white quartz sand [Cat. no. 27,473-9; $\rho_s = 2.4\,g\,cm^{-3}$; $D_p = 250\,\mu m$ (+50 −70 mesh)] with a thin, compact film of TiO_2 (by using Ti *t*-butoxide as precursor) in a vacuum-operated circulating fluidized bed reactor. Detailed information about the preparation method and catalyst characterization is given elsewhere [12]. The TiO_2 loading was determined by dissolving the films in a 10 wt.% solution of $(NH_4)_2SO_4$ in concentrated H_2SO_4 and subsequent quantification by elementary analysis. A digital Minolta, Dimage 7i-5.0 megapixel Model camera, coupled to an Universal Zeiss microscope, were used to analyze the quartz particle size distribution. A number of 110 micrographies were taken and a total of 584 particles were counted. The micrographies were processed with an ImageTool 3.0 program of the UTHSCSA software (Texas University). In Fig. 2 the particle size distribution of the quartz sand is presented as the percentage relative and accumulative frequency of the particle size intervals.

To investigate on the radiation field dependency with bed height owing to particle segregation in the FB, a radiation metering device was built to measure the light flux emerging from one window of the cell, as a function FB height, when the opposite windows was illuminated with one of the tubular black light lamps. A IL1700 radiometer, with a light SED005/WBS320/W sensor (a GaAsP type photodiode, 5 mm^2 of active area) was employed in the device. To allow measuring, the sensor was mounted on a vertical sliding support, parallel to the longitudinal axis of the cell, just by the light flux emerging window.

The photocatalytic activity of the composite was followed by monitoring the photodegradation of oxalic acid (Carlo Erba RSE, 99.9%) in water (45 ppm nominal concentrations); the solution was prepared using ultra pure water. The evolution of the oxalic concentration with time was followed with a 2020i model Dionex Ion Chromatograph equipped with an AS4A-SC analytic column. Steady state temperature and lamp operation conditions were set prior to initiating any experimental run.

3. The optical parameters as a function of position in the fluidized bed

In a fluidized bed containing a mixture of particles of different sizes, partial or complete segregation occurs, depending – primarily – on their dissimilar settling velocities. Hence, the modeling of the complete radiation field in the FB of our photocatalyst composite must take into account this segregation effect. For instance, changes in the solid hold-up will necessarily affect the local optical properties of the FB: one would expect that as the voidage of the fluidized bed increases in its upper zone (smallest particles prevail), the light energy will be able to penetrate further. Conversely, in the lowest region of

the FB, a lower voidage and a higher concentration of coarser particles will increase the light extinction, so that the depth of penetration of radiation will be lower [1,10]. Even more, local volumetric concentration of active catalyst (TiO_2) will also be dependent on composite particle size distribution, as a function of bed height.

In our previous work (Pozzo et al. [10]) it was found that the FB optical properties followed an inverse linear relationship with global bed expansion. Hence, the concept of specific spectral optical coefficients: k_λ^* and σ_λ^*, calculated at the central region of the FB for three different global bed expansions ($k_\lambda^* = k_\lambda E$ and $\sigma_\lambda^* = \sigma_\lambda E$), was utilized. By extending this concept of *specific* spectral coefficient to the *local* bed expansion E_h, an analogous correlation of optical properties with local voidage, can be expressed as

$$k_\lambda^* = k_\lambda E_h \quad \text{and} \quad \sigma_\lambda^* = \sigma_\lambda E_h, \quad \text{where } E_h = \frac{1-\varepsilon_o}{1-\varepsilon_h} \tag{1}$$

The local voidage at any bed position is a function of the FB particle size distribution. Two extreme, "border line" descriptions of the sedimentation mechanisms in a liquid FB of solid particles of multiple size, when all the solid particles are of the same density, have been proposed by Al-Dibouni and Garside [9]: (a) a perfect-size-classification model by which the bed can be described in terms of a series of horizontal plane segments with particles of a single size (or – more exactly – of an extremely narrow size range) and (b) a mixing model where it is assumed that an Eddy type of diffusion flux works against the segregation concentration gradient, making the bed nearly uniform with bed height.

In general, the opposite effects of classification and mixing interact to determine the overall behavior of fluidized beds containing a wide size distribution of particles. Al-Dibouni and Garside reported that the behavior of the bed is a function of ε, the overall FB voidage. According to them, a clear predominance of mixing appears when $0.65 < \varepsilon < 0.8$, but pronounced classification occurs for both, higher and lower values of ε. The calculated overall voidage in our system is $\varepsilon \approx 0.9$ (FB expansion = 7). Therefore, the simpler perfectly classified model is taken as a good approximation in the present case, to describe the FB particle distribution.

According to the perfectly classified bed model, the particle size group between D_p and $(D_p - dD_p)$ is contained in the bed region between heights h and $(h + dh)$. From this assumption they proposed the following differential expression:

$$\frac{dh}{dD_p} = \frac{m(D_p)}{A\rho_s[1-(U_o/U_t)]^{1/n}},$$

$$\text{where } n \text{ is given by } \frac{5.1-n}{n-2.7} = 0.1 Re_t^{0.9} \tag{2}$$

By numeric integration of Eq. (1) with the experimentally determined differential mass distribution of the solid composite, $m(D_p)$, a relationship between bed height and D_p can be found. Then, by using the following equation [13]:

$$U_o = U_t \varepsilon_h^n \tag{3}$$

and, by assuming that particles of any given size would produce a local voidage, ε_h equal to the one they would generate if they were the single particle size in the whole bed, a functionality between local voidage (ε_h) and bed height can be found [9].

4. The radiation field in the reaction volume

It is known that the total incident radiation ($G_{\lambda,\underline{x}}$) at any given position in a illuminated participative system can be calculated by solving the radiation transport equation (RTE), if the radiation boundary conditions and the spectral optical parameters (k_λ and σ_λ), as a function of position are known [14]. In our case, it can be expected that the radiation field will strongly vary both vertically along the FB (x direction), due to particle size anisotropy and transversally (y direction), because of the radiation extinction through the thickness of the reaction volume. By design, due to the uniformity of the incident radiation flux and the negligible incidence of border effects, no significant changes would occur instead, along the width (z direction, horizontal) of the reactor.

Thus, the RTE can be solved by modeling the radiation field as a two-dimensional (2D) system in a rectangular prismatic space confined between two parallel transparent optical windows, irradiated by the collimated radiation flux of the lamps. Hence, the propagation equation can be expressed as

$$\mu \frac{\partial I_\lambda(x,y,\underline{\Omega})}{\partial x} + \eta \frac{\partial I_\lambda(x,y,\underline{\Omega})}{\partial y} = -(\kappa_\lambda(x) + \sigma_\lambda(x)) I_\lambda(x,y,\underline{\Omega}) + \frac{\sigma_\lambda(x)}{4\pi} \int_{4\pi} p(\underline{\Omega}' \to \underline{\Omega}) I_\lambda(x,y,\underline{\Omega}')\, d\underline{\Omega}' \tag{4}$$

with the following boundary conditions:

at irradiated walls :

$$I_\lambda(x, y=0, \underline{\Omega} = \underline{\Omega}_{in}) = I^o_{\lambda,\underline{\Omega}} \text{ and}$$

$$I_\lambda(x, y=L_R, \underline{\Omega} = \underline{\Omega}_{in}) = I^o_{\lambda,\underline{\Omega}};$$

at non-illuminated areas :

$$I_\lambda(x=0, y, \underline{\Omega} = \underline{\Omega}_{in}) = 0 \text{ and}$$

$$I_\lambda(x=H_R, y, \underline{\Omega} = \underline{\Omega}_{in}) = 0 \tag{5}$$

By knowing the incident radiation flux on the reactor windows surface (measured by actinometry as described in Section 2), the angular distribution of a monochromatic incident radiation intensities on each point of the reactor windows ($I^o_{\lambda,\underline{\Omega}}$) can be obtained by adopting a three-dimensional source with superficial diffuse emission model (E-SDE Source Model) of the lamp-specular reflector system [14].

Since the lamp emission is polychromatic ($340 < \lambda < 400$ nm), its wavelength range was divided in 10 "quasi" monochromatic intervals. Besides, both the transmittance of the reactor windows and the reflectance of the parabolic reflectors were practically indifferent (gray) with respect to the radiation spectrum. So, the total average radiation flux obtained by actinometry was distributed among the wavelength intervals by just employing

the emission spectral profile of the lamp, in such a way that the sum of all the spectral fluxes resulted equal to the total emission flux. Thus, with the so calculated boundary conditions, defined by Eq. (5), the integro-differential Eq. (4), can be solved by using the discrete ordinate method (DOM). More details are given in Ref. [10].

Once the RTE is solved, the equation can be integrated to obtain the incident radiation at each point of the FB:

$$G_{(x,y)} = \int_{\lambda}\int_{\Omega} I_{\lambda(x,y,\underline{\Omega})}\,\mathrm{d}\Omega\,\mathrm{d}\lambda \cong \sum_{i=1}^{i=10}\int_{\Omega} I_{\lambda_i(x,y,\underline{\Omega})}\,\mathrm{d}\Omega \tag{6}$$

and the local volumetric rate of photon absorption (LVRPA = $e^{\mathrm{a}}_{(x,y)}$) can be calculated as

$$e^{\mathrm{a}}_{(x,y)} = \int_{\lambda}\int_{\Omega} k_{\lambda(x)} I_{\lambda(x,y,\underline{\Omega})}\,\mathrm{d}\Omega\,\mathrm{d}\lambda \cong \sum_{i=1}^{i=10}\int_{\Omega} k_{\lambda_i(x)} I_{\lambda_i(x,y,\underline{\Omega})}\,\mathrm{d}\Omega \tag{7}$$

Furthermore, and since even in a perfectly mixed reactor the LVRPA is non uniform in space, to obtain a global value of the reaction rate (to be compared with the observable one) for quantum efficiency calculation purposes, the volume averaged value (VRPA) of $e^{\mathrm{a}}_{(x,y)}$ should be determined as

$$\langle e^{\mathrm{a}}_{(x,y)}\rangle_{V_{\mathrm{R}}} = \frac{1}{V_{\mathrm{R}}}\int_{V_{\mathrm{R}}} e^{\mathrm{a}}_{(x,y)}\,\mathrm{d}V_{\mathrm{R}} \tag{8}$$

Finally, and by using this averaged value of the rate of photon absorption by the photoactive composite in the reaction volume, an *actual* intrinsic quantum yield (η) for the FB plane parallel reactor device can be calculated as follows:

$$\eta = \frac{\langle R^{\mathrm{O}}_{\mathrm{Ox}}(x,\,y)\rangle_{V_{\mathrm{R}}}}{\langle e^{\mathrm{a}}_{(x,y)}\rangle_{V_{\mathrm{R}}}} \tag{9}$$

5. The initial rate of the oxalic acid oxidation reaction

The decomposition of oxalic acid was conducted under the following design conditions: (a) hydrodynamic and thermal steady state, (b) perfect mixing in the recirculating system, outside the reactor cell and inside the FB, (c) negligible volume of the connecting lines and (d) zero reaction rate outside the illuminated reaction volume. For an initial oxalic acid concentration of 45 ppm a pseudo-zero-order-reaction rate can be assumed [15]. Furthermore, the system was always operated as a continuous differential reactor inside a loop of a batch recirculating system so that the mass balance equation for the organic substrate can be formalized as [15]:

$$\frac{\mathrm{d}C_{\mathrm{Ox}}(t)}{\mathrm{d}t} = \frac{V_{\mathrm{R}}}{V_{\mathrm{T}}}\langle R_{\mathrm{Ox}}(x,\,y,\,t)\rangle_{V_{\mathrm{R}}} \tag{10}$$

Within the range of validity of a pseudo-zero order-reaction rate, Eq. (9) can be immediately integrated, with just the initial condition: $C_{\mathrm{Ox}}(t=0) = C^{\mathrm{O}}_{\mathrm{Ox}}$, to yield initial rate data:

$$\langle R^{\mathrm{O}}_{\mathrm{Ox}}(x,\,y)\rangle_{V_{\mathrm{R}}} = \frac{V_{\mathrm{T}}}{V_{\mathrm{R}}}\left(\frac{C_{\mathrm{Ox}}(t) - C^{\mathrm{O}}_{\mathrm{Ox}}}{t - t_{\mathrm{O}}}\right) \tag{11}$$

More details about this data treatment are given in Ref. [15].

6. Results and discussion

The experimental and model-estimated relative transmittance values of the FB, as a function of bed height, are presented in Fig. 3. Here, the relative transmittance ($T/T_{\max}$) is defined as the ratio between the FB transmittance at any given bed height (T_h) and that of pure water filling the reactor space ($T_{\max}$). The experimental values of transmittance were measured as described in Section 2 of the present work; the estimated values were calculated by numerical integration of the radiation transfer equation. For each height of the FB, the discrete ordinate method in an unidirectional and uni-dimensional model (1DD) was used for the calculations. More details are given in [10]. The corresponding local optical parameters for the computations were obtained from the perfectly classified model for the FB, as described in Section 3. For illustration purposes, the calculated values of local bed voidage are also plotted in Fig. 3.

As it can be readily appreciated, both the estimated and experimental values of the relative transmittance ($T/T_{\max}$) are quite close, validating the model assumptions. Therefore, the relationships found among the local and specific optical coefficients, and FB voidage versus bed position (Eq. (1)), were used to determine the radiation field profile in the fully illuminated photoreactor volume.

In Fig. 4a, the total local incident radiation ($G_{x,y}$) is presented as a function of FB height (x) and thickness (y). For any given thickness, the local values of the incident radiation

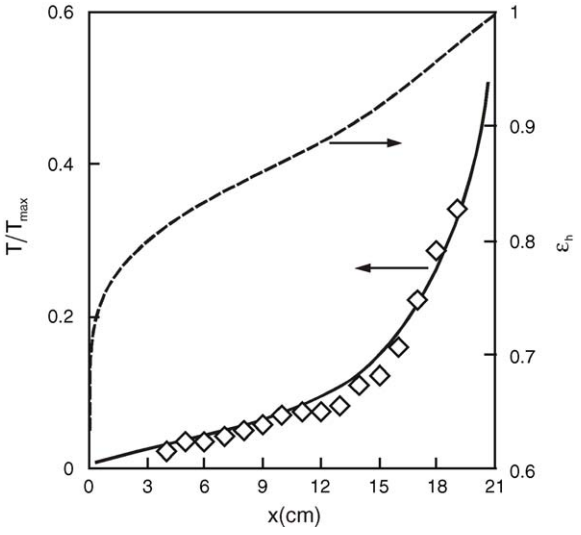

Fig. 3. Local bed voidage (ε_h) and relative transmittance: experimental (◊) and calculated (line), as a function of FB height. The ε_h value*s* were calculated as described in the text (Eq. (3)). The experimental transmittance values are the average of triplicate measurements, for each height; the maximum dispersion among values was <5%.

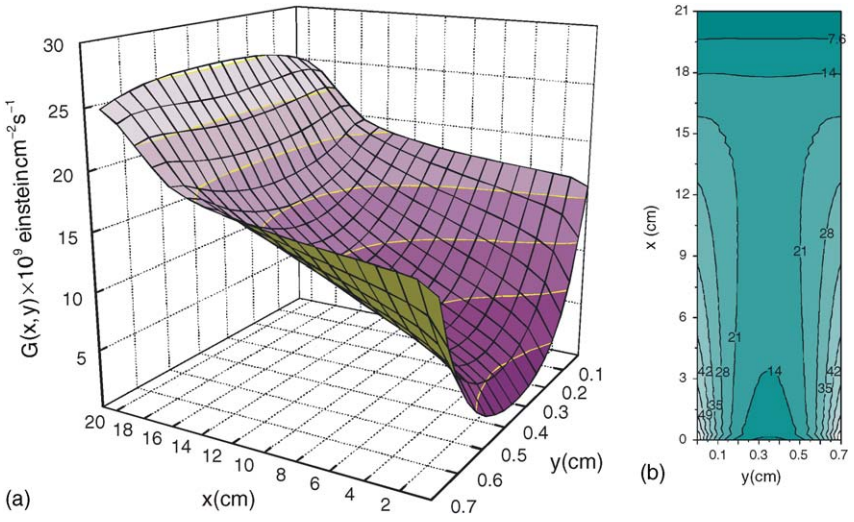

Fig. 4. (a) Total local incident radiation ($G_{x,y}$), and (b) local volumetric rate of radiation energy absorption per unit volume of the FB ($e^{a}_{x,y}$), $\times 10^9$ Einstein cm^{-3} s^{-1}, as a function of FB height (x) and thickness (y).

increase monotonically in the upward direction. Across the bed (y direction), for any given height, the concave parabolic-like profiles of $G_{x,y}$ reveal how vastly the incoming radiation interacts with the absorbing media right upon entering through the reactor walls, where it is at its maximum value.

By looking now to the level curves of Fig. 4b, which represent iso-absorption zones inside the reactor, we can observe that the decrease in radiation absorption rate away from the reactor walls is abrupt. Moreover, it is also evident, then, that $e^{a}_{(x,y)}$ *diminishes* with bed height, even though the available radiation actually increases upwards. This apparent contradiction can be fully explained as due to the lessening in concentration of the light-absorbing, active material at higher bed positions, since (as shown in Fig. 3) the FB voidage increases in the x direction. Therefore, a compromise between increasing radiation extinction and more effective energy absorption with higher active material concentrations, and vice versa, determine the profile of the local energy absorption rate depicted in Fig. 4b. The observable reactivity in the device, which is correlated with the volume-averaged value of $e^{a}_{(x,y)}$ (VRPA), is indeed caused by the convolution of two highly anisotropic (radiation and bed voidage) scalar fields. The calculated intrinsic efficiency of the FB reactor, according to Eq. (9), was $\eta = 0.37$, a fairly remarkable figure when compared to other devices.

7. Conclusions

Using a model contaminant (oxalic acid), it was shown that a fluidized bed of a composite of titania-coated quartz sand (by plasma-CVD) could be a sound alternative to TiO_2 slurried systems for the photo-oxidation of organic water pollutants. The local volumetric optical properties (spectral absorption and scattering coefficients) necessary for the description and evaluation of the radiation field inside the reaction volume (a requirement for a significant calculation of photocatalytic efficiencies) can be successfully obtained as a function of bed height, by assuming completely segregated FB. The total local incident radiation at each point in the FB, and the corresponding local volumetric rate of photon absorption (LVRPA) can also be determined by a proper solution of the spectrum-resolved integro differential radiation transfer equation using a two-dimensional model. The calculated intrinsic efficiency of a FB plane reactor device was quite high as compared to other similar devices with slurried photocatalyst. The intrinsic efficiency was defined as the ratio between the reaction volume-averaged values of both, the rate of photocatalytic decomposition of oxalic acid and the LVRPA. The particular distribution profile of the radiation field inside the FB, conforming a fully illuminated-participating reaction volume, seems to play a decisive role on the singular performance of this photocatalytic device.

Acknowledgements

The authors thank the financial support from the Consejo Nacional de Investigaciones Científicas y Técnicas (CONICET), Universidad Nacional del Litoral (UNL) and ANPCyT of Argentina. Thanks are also given to Eng. Claudia Romani and to Elvio Martínez for their skilled technical assistance.

References

[1] D. Iatridis, P.L. Yue, The absorption of light energy in flat fluidized photoreactors, Chem. Eng. J. 45 (1990) 1–8.
[2] L. Rizzuti, A. Brucato, D. Iatridis, P.L. Yue, Light transmittance and reflectance of flat fluidized photoreactors, Chem. Biochem. Eng. Quart. 77 (1992) 19–23.
[3] L. Rizzuti, A. Brucato, D. Iatridis, P.L. Yue, Modelling of light transmittance and reflectance in flat fluidized photoreactors, Can. J. Chem. Eng. 70 (1992) 1063–1070.
[4] A. Bhargava, M.F. Kabir, E. Vaisman, C. Langford, A. Kantzas, Novel technique to characterize the hydrodynamics and analyze the performance of a fluidized-bed photocatalytic reactor for wastewater treatment, Ind. Eng. Chem. Res. 43 (2004) 980–989.
[5] S.C. Kennedy, R.H. Bretton, Axial dispersion of spheres fluidized with liquids, AIChE J. 12 (1) (1966) 24–30.

[6] A.P. Van der Meer, C.M. Blanchard, J.A. Wesselingh, Mixing of particles in liquid fluidized beds, Chem. Eng. Res. Des. 62 (1984) 214–222.
[7] B.K. Dutta, S. Bhattacharya, S.K. Chaudhary, B. Barman, Mixing and segregation in a liquid fluidized bed of particles with different size and density, Can. J. Chem. Eng. 66 (1988) 676–680.
[8] R. Di Felice, L.-G. Gibilaro, S.P. Waldran, Mixing and segregation in binary-solid liquid fluidized beds, Chem. Eng. Sci. 42 (4) (1987) 639–652.
[9] M.R. Al-Dibouni, J. Garside, Particle mixing and classification in liquid fluidized beds, Trans. I. Chem. Eng. 57 (1979) 94–103.
[10] R.L. Pozzo, R.J. Brandi, J.L. Giombi, M.A. Baltanás, A.E. Cassano, Design of fluidized bed photoreactors: optical properties of photocatalytic composites of titania CVD-coated onto quartz sand, Chem. Eng. Sci. 60 (2005) 2785–2794.
[11] R.L. Pozzo, M.A. Baltanás, A.E. Cassano, Towards a precise assessment of the performance of supported photocatalysts for water detoxification processes, Catal. Today 54 (1) (1999) 143–157.
[12] M. Morstein, M. Karches, R.L. Pozzo, J.L. Giombi, M.A. Baltanás, Plasma-CVD-coated glass beads as photocatalyst for water decontamination, Catal. Today 72 (3/4) (2002) 267–279.
[13] J.F. Richardson, W.N. Zaki, Sedimentation and fluidization in solid-liquid systems. Part I, Trans. I. Chem. Eng. 32 (1954) 35–53.
[14] A.E. Cassano, C.M. Martín, R.J. Brandi, O.M. Alfano, Photoreactor analysis and design: fundamentals and applications, Ind. Eng. Chem. Res. 34 (1995) 2166–2201.
[15] R.L. Pozzo, J.L. Giombi, M.A. Baltanás, A.E. Cassano, The performance in a fluidized bed reactor of photocatalysts immobilized onto inert supports, Catal. Today 62 (2000) 175–187.